NASA/CR—2001-210710

Mars Flyer Rocket Propulsion Risk Assessment
Kaiser Marquardt Testing

Kaiser Marquardt
Van Nuys, California

April 2001

The NASA STI Program Office . . . in Profile

Since its founding, NASA has been dedicated to the advancement of aeronautics and space science. The NASA Scientific and Technical Information (STI) Program Office plays a key part in helping NASA maintain this important role.

The NASA STI Program Office is operated by Langley Research Center, the Lead Center for NASA's scientific and technical information. The NASA STI Program Office provides access to the NASA STI Database, the largest collection of aeronautical and space science STI in the world. The Program Office is also NASA's institutional mechanism for disseminating the results of its research and development activities. These results are published by NASA in the NASA STI Report Series, which includes the following report types:

- TECHNICAL PUBLICATION. Reports of completed research or a major significant phase of research that present the results of NASA programs and include extensive data or theoretical analysis. Includes compilations of significant scientific and technical data and information deemed to be of continuing reference value. NASA's counterpart of peer-reviewed formal professional papers but has less stringent limitations on manuscript length and extent of graphic presentations.

- TECHNICAL MEMORANDUM. Scientific and technical findings that are preliminary or of specialized interest, e.g., quick release reports, working papers, and bibliographies that contain minimal annotation. Does not contain extensive analysis.

- CONTRACTOR REPORT. Scientific and technical findings by NASA-sponsored contractors and grantees.

- CONFERENCE PUBLICATION. Collected papers from scientific and technical conferences, symposia, seminars, or other meetings sponsored or cosponsored by NASA.

- SPECIAL PUBLICATION. Scientific, technical, or historical information from NASA programs, projects, and missions, often concerned with subjects having substantial public interest.

- TECHNICAL TRANSLATION. English-language translations of foreign scientific and technical material pertinent to NASA's mission.

Specialized services that complement the STI Program Office's diverse offerings include creating custom thesauri, building customized data bases, organizing and publishing research results . . . even providing videos.

For more information about the NASA STI Program Office, see the following:

- Access the NASA STI Program Home Page at ***http://www.sti.nasa.gov***

- E-mail your question via the Internet to help@sti.nasa.gov

- Fax your question to the NASA Access Help Desk at 301–621–0134

- Telephone the NASA Access Help Desk at 301–621–0390

- Write to:
  NASA Access Help Desk
  NASA Center for AeroSpace Information
  7121 Standard Drive
  Hanover, MD 21076

NASA/CR—2001-210710

Mars Flyer Rocket Propulsion Risk Assessment
Kaiser Marquardt Testing

Kaiser Marquardt
Van Nuys, California

Prepared under Contract NAS3–99198

National Aeronautics and
Space Administration

Glenn Research Center

April 2001

Available from

NASA Center for Aerospace Information
7121 Standard Drive
Hanover, MD 21076
Price Code: A03

National Technical Information Service
5285 Port Royal Road
Springfield, VA 22100
Price Code: A03

Available electronically at http://gltrs.grc.nasa.gov/GLTRS

TABLE OF CONTENTS

LIST OF FIGURES

LIST OF TABLES

LIST OF NOMENCLATURE

Symbols

C^*	characteristic velocity
δ	ignition delay
F, FT	thrust (vacuum, unless otherwise specified)
η_{C^*}	C* efficiency
I_{sp}, ISP	specific impulse (vacuum, unless otherwise specified)
N_2O_4	dinitrogen tetroxide
NO	nitric oxide
O/F	oxidizer-to-fuel mixture ratio
p_{cell}, PCELL	test cell pressure
p_{mf}, PMF	fuel inlet manifold pressure
p_{mo}, PMO	oxidizer inlet manifold pressure
t	time
T_{c1}, TC1	injector-chamber interface temperature #1
T_{c2}, TC2	injector-chamber interface temperature #2
T_{ch}, TCH	chamber temperature
T_{mf}, TMF	fuel inlet manifold temperature
T_{mo}, TMO	oxidizer inlet manifold temperature
t_{off}	valve time off
t_{on}	valve time on
T_{f1}, TF1	oxidizer-side valve flange temperature
T_{f2}, TF2	fuel-side valve flange temperature
T_{vf}, TVF	fuel-side valve temperature
T_{vo}, TVO	oxidizer-side valve temperature
I_V, VI	valve current
V_V, VV	valve voltage
w_{fu}, WFU	fuel flow rate
w_{ox}, WOX	oxidizer flow rate

Acronyms

ACC1	accelerometer #1
C-103	columbium-metal alloy
CD-ROM	compact disc read-only memory
GN2	gaseous nitrogen
LN2	liquid nitrogen
MMH	monomethylhydrazine
MON-25	mixed oxides of nitrogen, 75% N2O4 / 25% NO by weight
MON-3	mixed oxides of nitrogen, 97% N2O4 / 3% NO by weight
NASA	National Aeronautics and Space Administration
RAM	random-access memory
SCXI	National Instruments signal conditioning system

1 INTRODUCTION

The Mars Flyer mission proposed by the National Aeronautics and Space Administration will fly a miniature airplane in the Martian atmosphere on the centennial anniversary of the Wright brother's first powered flight. At the time of proposal, both, an electric motor-driven propeller and a chemical rocket engine were under consideration for the Mars Flyer propulsion system. As part of a risk reduction investigation, Kaiser Marquardt was contracted to validate, by test demonstration, the use of a chemical thruster utilizing mixed oxides of nitrogen and monomethylhydrazine. The objective was to provide NASA with as much data as possible for the flight system decision.

Preliminary studies performed by NASA showed that a thrust level of 8.9 N would be appropriate for a rocket-powered Mars Flyer. The Mars Flyer will be power-limited and volume-limited, therefore, the rocket propulsion system will have to employ storable propellants and be capable of operating in the Martian environment without thermal management. Without thermal management, the entire propulsion system, including propellants, will be subjected to extremely low temperatures as the average diurnal temperature of the surface-level Martian atmosphere is –40 degrees Celsius.

An experimental investigation was conducted to assess the performance of an 8.9-N, bipropellant thruster operating at –40 °C with monomethylhydrazine (MMH) and mixed oxides of nitrogen (MON). To facilitate engine operation at low temperatures, dinitrogen tetroxide, N_2O_4, was saturated with nitric oxide, NO, to lower the freezing point. The freezing point of the industry-standard, 3% nitric oxide in dinitrogen tetroxide (MON-3) is -15 °C. By increasing the nitric oxide content to 25% (MON-25), the freezing point was lowered to –55 °C, thus enabling safe operation of the thruster at –40 °C with sufficient margin for error. The thruster was tested in a near-vacuum environment and conditioned, along with the propellants, to –40 °C prior to hot firing. Thruster operating parameters included oxidizer-to-fuel mixture ratios of 1.6 to 2.7 and inlet pressure ranging from 689 to 2070 kPa. The test matrix consisted of many 10-second firings and several 60, 300, 600, and 1200-second firings. Measurements included thrust, propellant flow rates, propellant inlet pressures and temperatures, engine temperatures, system vibrations, and valve control-signal characteristics. Data obtained from testing were analyzed to determine engine performance characteristics such as ignition delay, specific impulse, I_{sp}, versus oxidizer-to-mixture ratio, O/F, I_{sp} versus thrust, F, and the vibration frequency spectrum. Preliminary results indicate that the additional nitric oxide not only permits lower propellant temperatures, but also compensates for the loss of performance associated with the lower propellant temperatures by introducing additional chemical energy to the combustion process. Results exhibited comparable, if not superior, performance as compared to those obtained with the same thruster fired at normal operating temperatures (~22 °C) using MON-3 and MMH.

2 TEST PROGRAM

2.1 Test Article

The test article used in this investigation was the Kaiser Marquardt Model R-53 8.9-N bipropellant thruster shown in Figure 1. The thruster consists of three primary components, the control valve, the propellant injector, and the chamber-nozzle assembly. The engine control valve is a Moog torque-motor bipropellant type designed to simultaneously control the flow of both oxidizer and fuel. The injector consists of a single unlike-doublet with two separate injection ports for fuel-film cooling of the combustion chamber wall. The portion of fuel used for fuel-film cooling was, by design, to be 30% of the total flow. As a result of manufacturing difficulties, however, the cooling fuel was only

20% of the total flow, which resulted in significantly higher chamber temperatures during hot firing. The single unlike-doublet is a pair of injection ports designed to impinge a stream of oxidizer with a stream of fuel inside the combustion chamber and very near the external face of the injector (see schematic shown in Figure 2). The chamber-nozzle assembly consists of a single piece of forged C-103 columbium (niobium) alloy with a silicide coating to prevent oxidation. In these tests, the chamber was operated at temperatures of up to 1500 °C for a total of nearly 10,000 seconds.

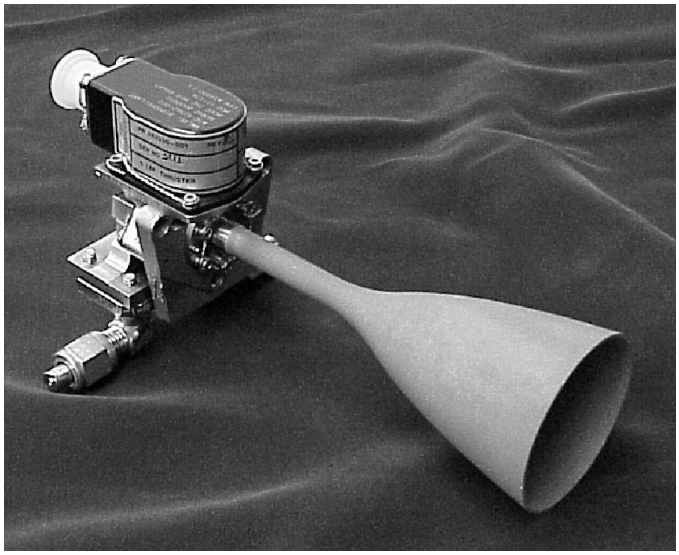

Figure 1 Kaiser Marquardt Model R-53 8.9-N bipropellant thruster

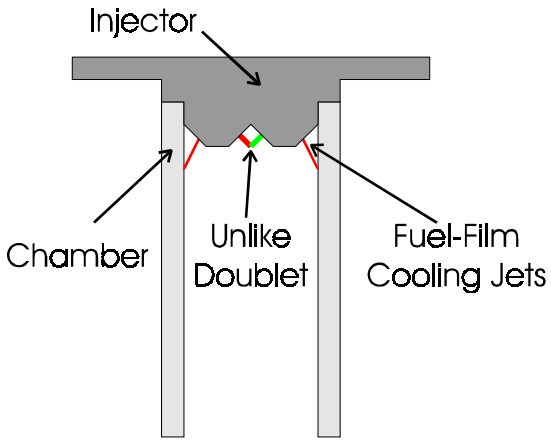

Figure 2 R-53 propellant injection and fuel-film cooling scheme.

2.2 Test Facilities

All testing was conducted in Cell 9 of the Kaiser Marquardt Rocket Test Facility located in Van Nuys, California and shown in Figure 3. The Cell 9 Rocket Test Facility includes a small thrust stand (see Figure 4) located within a very large vacuum sphere (see Figure 3). The vacuum sphere may be evacuated using a large steam ejection system or a series of Stokes pumps and Roots blowers shown in Figure 5. The facility is fully automated and operated from a remote data acquisition and control center shown in Figure 6. Data acquisition was performed using a National Instruments SCXI signal conditioning system controlled by an Intel Pentium II 500 MHz computer having 1 gigabyte of RAM,

an 18 gigabyte hard drive, a 53-cm monitor, and a CD-ROM writer. The MON-25 propellant was produced on-site and analyzed in the Kaiser Marquardt chemistry lab.

Figure 3 Kaiser Marquardt Cell 9 rocket test facility.

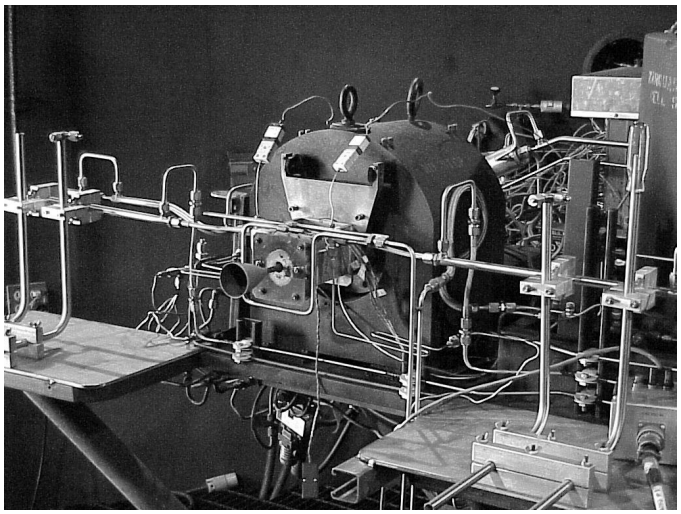

Figure 4 R-53 thruster mounted on Cell 9 small rocket thrust stand.

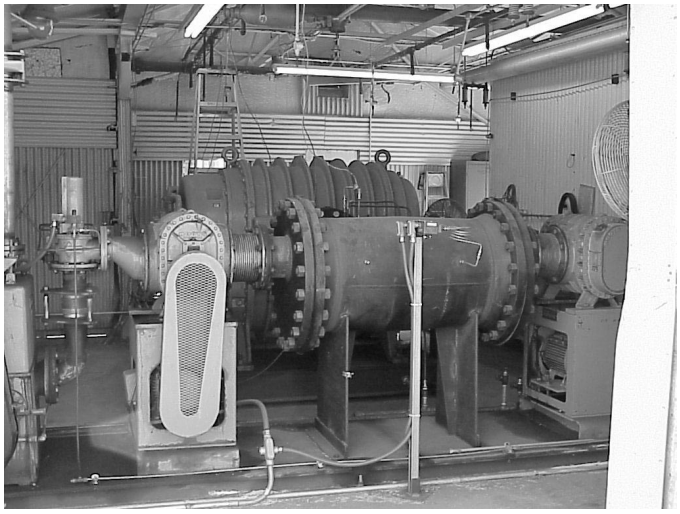

Figure 5 Roots blowers and Stokes pumps for cell evacuation.

Figure 6 Cell 9 data acquisition and facility control center.

2.3 Facility Modifications

To accommodate testing of the Model R-53 8.9-N thruster at –40 °C, it was necessary to modify the existing propellant conditioning system and to make provisions for thermal conditioning of the thruster hardware. Normally, propellants are conditioned using an Environmental Industries (EI) Model ME2110 refrigeration system. This system, however, is only capable of conditioning propellants to –7 °C. Therefore, a Government-supplied thermal conditioning system consisting of two FTS Model RC10B0, shown in Figure 7, was used in conjunction with the existing system. This combination system enabled conditioning of the propellants to temperatures below –46 °C.

Conditioning of the propellants was achieved using a system of co-annular plumbing, where the propellants were passed through an interior passage encased in an outer tube of flowing refrigerant. This system of co-annular plumbing began at the main propellant run tanks, extended to the engine valve inlets, and was interrupted only by those transition joints and valves where the system could not be practically implemented. Conditioning was divided into two stages. The first stage utilized the

normal EI refrigeration system with ethylene glycol as the refrigerant and the second stage utilized the FTS refrigeration system with a silicon-based refrigerant. The first stage conditioned the propellants in the storage tanks and in the lines up to the cell vacuum sphere. The second stage conditioned the propellants from just inside the cell wall up to the engine inlets. The first stage temperature was controlled at –7 °C, while the second stage temperature was set at the desired run temperature of down to –40 °C.

To provide a stable propellant temperature throughout the duration of hot firings, lasting up to 20 minutes, one-gallon, chilled accumulator tanks were installed serially in-line with the propellant supply lines. These tanks were located inside the cell vacuum sphere and controlled with the second-stage thermal conditioning system. This arrangement provided a buffer between the propellant chilled to the desired run temperature and the higher-temperature propellant entering from outside the cell vacuum sphere.

Figure 7 FTS Model RC10B0 refrigeration units in protective shed.

The engine hardware was conditioned to –40 °C on the thrust stand through the use of a nitrogen gas purge. Liquid nitrogen was circulated through a reservoir, which contained a helical heat exchanger tube through which gaseous nitrogen was passed. The cold gaseous nitrogen was introduced to the engine hardware through a system of normal impingement jets shown in Figure 8. A ring containing several jet orifices cooled the engine valve, injector, and chamber. A bar, also containing several jet orifices, cooled the engine inlets and the short sections of unconditioned, flexible propellant lines. Figure 9 shows a schematic of the entire setup including the propellant and engine hardware conditioning systems.

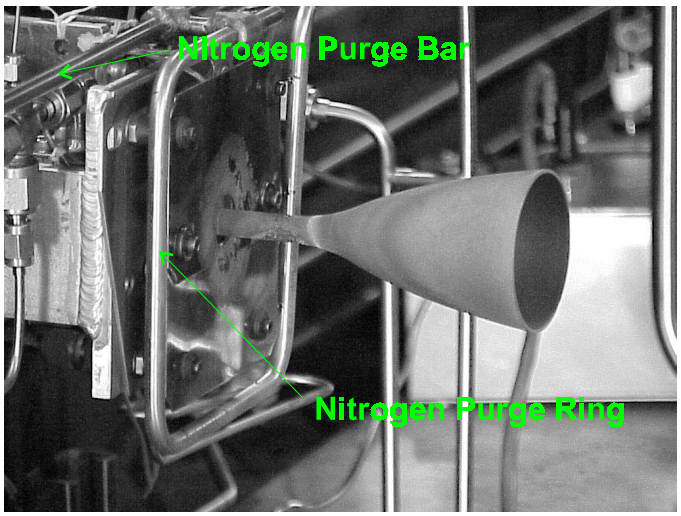

Figure 8 Nitrogen purges for engine thermal conditioning.

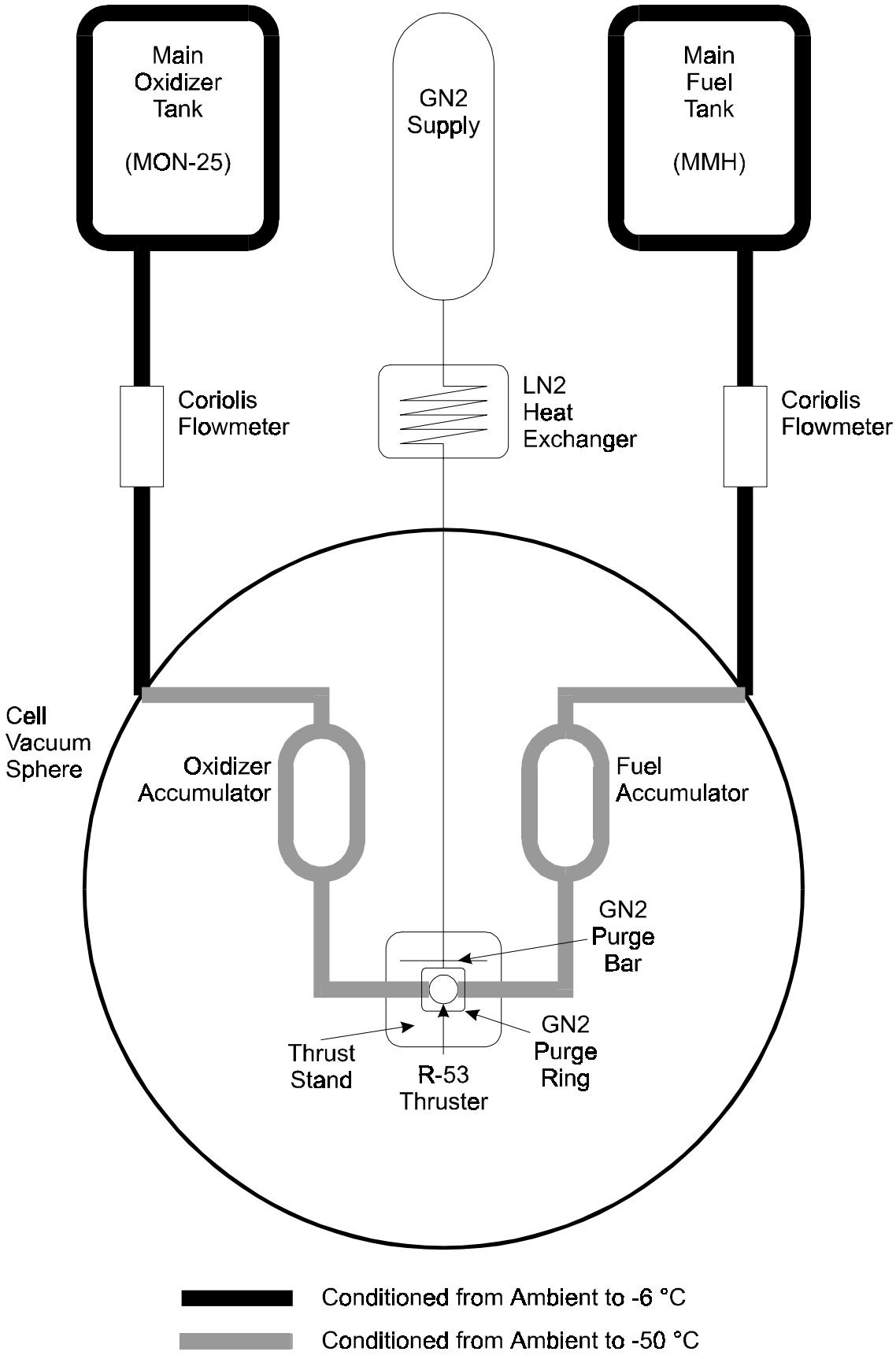

Figure 9 Facility Flow Schematic for Mars Flyer Testing

2.4 MON-25 Production

The required mixed oxides of nitrogen composition, 75% dinitrogen tetroxide (N_2O_4) and 25% nitric oxide (NO) by weight, was produced on-site at Kaiser Marquardt. Production was achieved by introducing gaseous NO to commercially available MON-3 (3% NO in N_2O_4) in a controlled reaction. Production began with a known amount of MON-3 in the run-storage tank. Nitric oxide was then allowed to flow into the run-storage tank from an external storage cylinder mounted on a weight balance. Because the saturation of NO into N_2O_4 involves an exothermic reaction, the flow of the nitric oxide was carefully controlled so as to preclude thermal run-away. The storage tank was conditioned to –7 °C to lower the vapor pressure of the mixture and to accelerate the process. For reference, Figure 10 shows the vapor pressure of the mixed oxides of nitrogen. A tank stirring mechanism was also used to further accelerate the process. After the required amount of NO had been transferred and the saturation process was complete, a sample was taken for composition analysis. The species composition analysis was performed in the Kaiser Marquardt chemistry laboratory and according to specification MIL-PRF-26539E. After completion of production, the storage tank was held under pressure (> 700 kPa) to ensure composition continuity. This also permitted shutdown of the thermal conditioning system during storage.

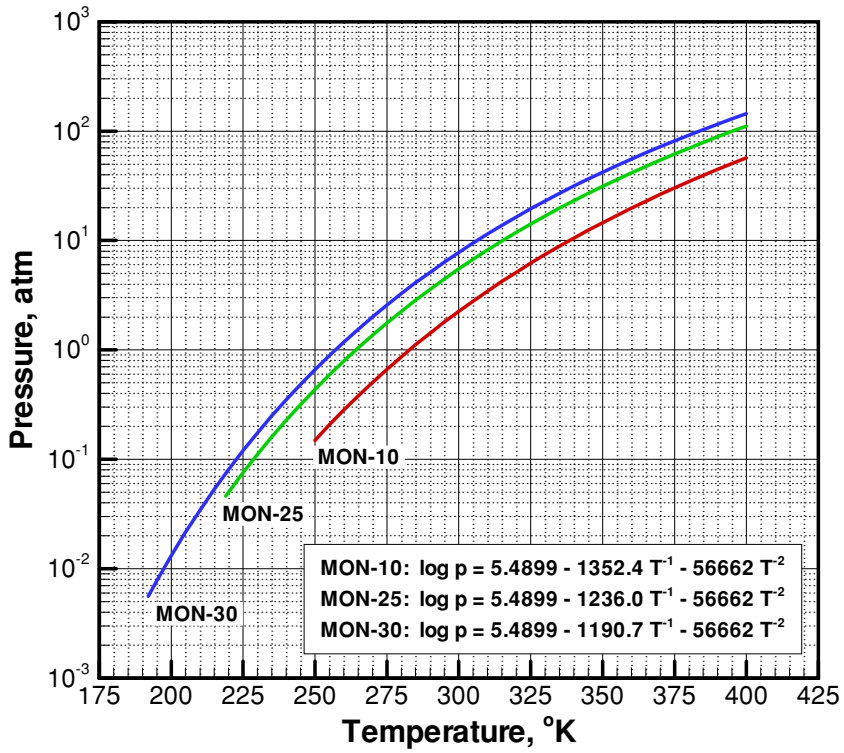

Figure 10 Vapor pressure of the mixed oxides of nitrogen.

2.5 Instrumentation and Data Acquisition

In addition to the standard facility instrumentation, the engine test setup was equipped with instrumentation to measure thrust, propellant flow rates, propellant inlet pressures, propellant inlet temperatures, valve control signal characteristics, various engine temperatures, and system vibrations. All measurements were calibrated in standard (English) units and later converted to metric (System International) units. Table 1 shows a summary of the engine test setup-specific instrumentation along

with the ranges of interest. Figure 11 shows the locations of all engine thermocouples. Data acquisition was performed using a National Instruments SCXI signal conditioning system controlled by an Intel Pentium II 500 MHz computer having 1 gigabyte of RAM, an 18 gigabyte hard drive, a 53-cm monitor, and a CD-ROM writer.

Table 1 Engine Test Setup-Specific Instrumentation

MEASUREMENT	ACRONYM	UNITS	MIN	MAX	CUT
Fuel Flow Rate	WFU	lbm/sec	0.002	0.01	
Oxidizer Flow Rate	WOX	lbm/sec	0.002	0.01	
Thrust	FT	lbf	0	5	
Fuel Inlet Manifold Pressure	PMF	psia	0	300	
Oxidizer Inlet Manifold Pressure	PMO	psia	0	300	
Cell Pressure	PCELL	psia	0	1.0	
Valve Voltage	VV	volts	0	50	
Valve Current	VI	amps	0	1	
Fuel Inlet Manifold Temperature	TMF	°F	-60	120	
Oxidizer Inlet Manifold Temperature	TMO	°F	-60	120	
Chamber Temperature	TCH	°F	1500	3000	2800 max
Injector/Chamber Temperature	TC1	°F	-60	1000	800 max
Injector/Chamber Temperature	TC2	°F	-60	1000	800 max
Valve Temperature - Fuel Side	TVF	°F	-60	500	250 max
Valve Temperature - Oxidizer Side	TVO	°F	-60	500	250 max
Flange Temperature	TF1	°F	-60	1000	250 max
Flange Temperature	TF2	°F	-60	1000	250 max
Accelerometer	ACC1	g	-100	+100	

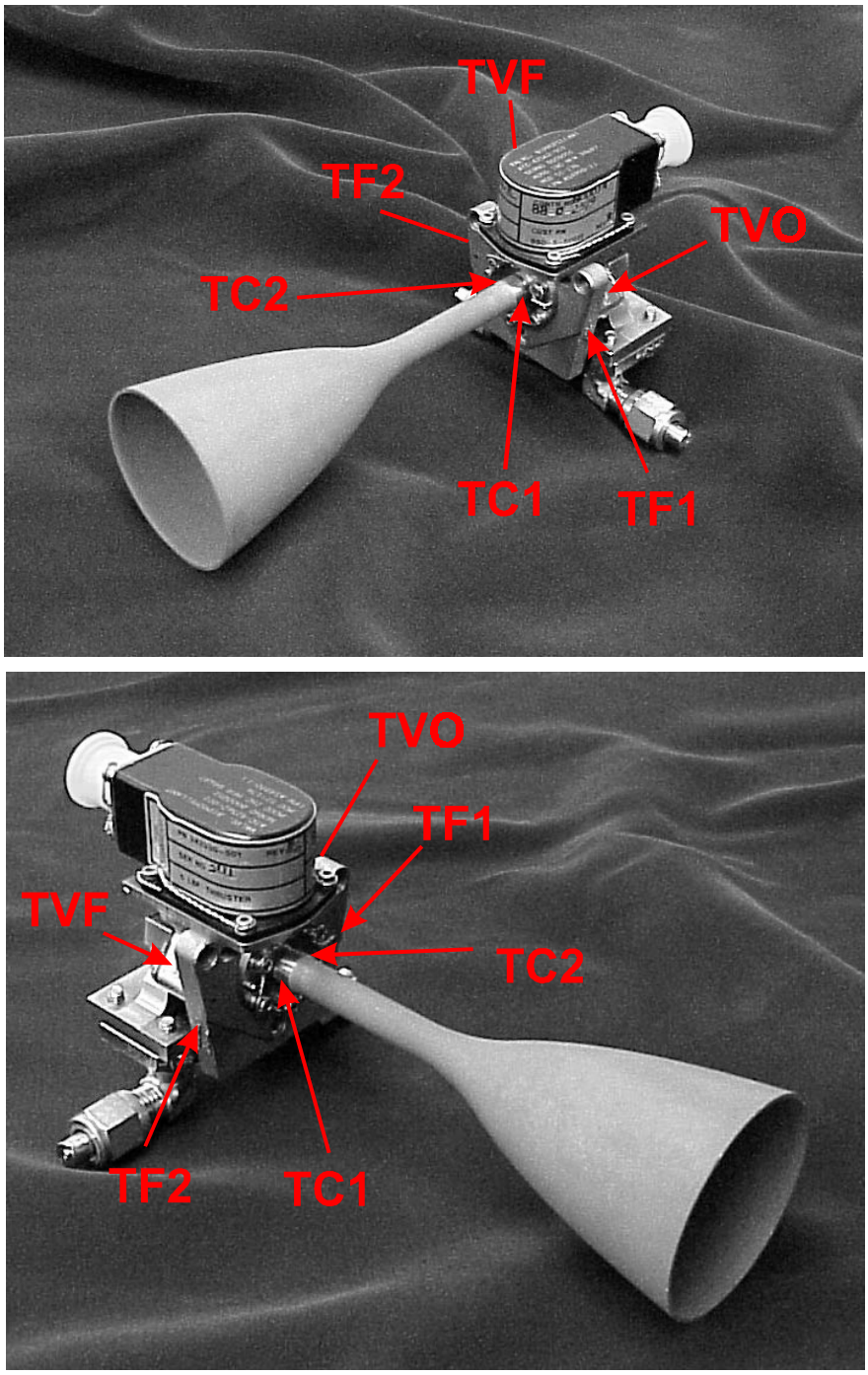

Figure 11 Engine thermocouple locations.

3 RESULTS AND DISCUSSION

The thruster was tested with propellant inlet pressures ranging from 723 to 2315 kPa, yielding vacuum thrust levels of 4.5 to 10.6 N with mixture ratios from 1.6 to 2.7. Table 2 shows a summary of the tests performed.

Table 2 Actual Test Matrix Performed

RUN	p_{mo}	p_{mf}	t_{ON}	t_{OFF}	PULSES	t_{prop}	p_{cell}
	kPa	kPa	sec	sec		°C	kPa
688	1571	1565	10	---	1	-40	< 0.15
689	1570	1555	10	---	1	-40	< 0.15
690	1567	1586	10	---	1	-40	< 0.15
691	1566	1658	10	---	1	-40	< 0.15
692	1564	1795	10	---	1	-40	< 0.15
693	1543	1836	10	---	1	-40	< 0.15
694	1549	1828	10	---	1	-40	< 0.15
695	1550	1904	10	---	1	-40	< 0.15
696	1576	2022	10	---	1	-40	< 0.15
697	1522	2076	10	---	1	-40	< 0.15
698	1479	2108	10	---	1	-40	< 0.15
699	1447	2134	10	---	1	-40	< 0.15
700	1449	2177	10	---	1	-40	< 0.15
701	1621	1766	10	---	1	-40	< 0.15
702	1657	1729	10	---	1	-40	< 0.15
703	1657	1693	10	---	1	-40	< 0.15
704	1657	1624	10	---	1	-40	< 0.15
705	1695	1559	10	---	1	-40	< 0.15
706	1727	1591	10	---	1	-40	< 0.15
707	1824	1629	10	---	1	-40	< 0.15
708	1553	1835	10	---	1	-40	< 0.15
709	1696	1971	10	---	1	-40	< 0.15
710	1861	2108	10	---	1	-40	< 0.15
711	1967	2248	10	---	1	-40	< 0.15
713	2028	2315	10	---	1	-40	< 0.15
714	1407	1697	10	---	1	-40	< 0.15
715	1306	1555	10	---	1	-40	< 0.15
716	1202	1416	10	---	1	-40	< 0.15
717	1072	1278	10	---	1	-40	< 0.15
718	929	1105	10	---	1	-40	< 0.15
719	792	963	10	---	1	-40	< 0.15
720	723	848	10	---	1	-40	< 0.15
721	1551	1831	10	---	1	-40	< 0.15
722	1544	1828	300	---	1	-40	< 0.15
726	1564	1839	10	---	1	-7	< 0.15
727	1555	1831	10	---	1	-7	< 0.15
728	1607	1758	10	---	1	-7	< 0.15
729	1556	1836	10	---	1	-18	< 0.15
730	1553	1827	10	---	1	-18	< 0.15
733	1566	1838	10	---	1	-18	< 0.15
735	1552	1835	0.1	0.1	20	-40	< 0.15
736	1551	1828	0.1	0.1	20	-40	< 0.15
737	1551	1825	0.1	0.1	20	-40	< 0.15
739	1551	1827	1200	---	1	-40	< 0.15
740	1551	1827	1200	---	1	-40	< 0.15
741	1547	1826	60	---	1	-40	1.5
742	1551	1827	1200	---	1	-40	< 0.15
743	1519	1853	1200	---	1	-40	< 0.15
744	1528	1827	600	---	1	-40	< 0.15
745	1520	1819	600	---	1	-40	< 0.15
746	1533	1820	600	---	1	-40	< 0.15
747	1536	1820	300	---	1	-40	< 0.15
748	1540	1826	300	---	1	-40	< 0.15
749	1530	1828	300	---	1	-40	< 0.15
750	1551	1827	300	---	1	-40	< 0.15

Initial tests were performed to ascertain the propellant inlet pressure producing a vacuum thrust level, F_{vac}, of 8.9 N and an oxidizer-to-fuel mixture ratio, O/F, of 2.1. The engine was designed to produce these nominal values for equal inlet pressures of 1517 kPa. Improper propellant-flow trim orifices, however, required oxidizer and fuel inlet pressures of 1551 and 1827 kPa, respectively, to produce the nominal performance.

Measurements included thrust, propellant flow rates, propellant inlet pressures and temperatures, engine temperatures, system vibrations, and valve control-signal characteristics. Data obtained from testing were analyzed to determine engine performance characteristics such as ignition delay, specific impulse, I_{sp}, versus oxidizer-to-mixture ratio, O/F, I_{sp} versus thrust, F, and the vibration frequency spectrum. In each firing, 1 second of pre-fire data was taken to obtain an accurate pre-run thrust tare and to ensure that all instrumentation was operating properly prior to firing. In each case, 10 seconds of data was taken after the hot firing to obtain a post-run thrust tare and to observe thermal soak back trends.

The total firing time for the matrix described in Table 2 is nearly 8600 seconds. Although the amount of fuel-film cooling was much less than the design value, resulting in very high chamber temperatures, the engine did survive the entire test matrix. In fact, an additional 2400 seconds of firing time were put on the engine to dispose of the excess propellants. Record of these final runs was not possible, because the remaining propellant was downstream of the flow meters.

3.1 Ignition Characteristics

Ignition delay was measured as the time between control signal "ON" and the first instance of measurable thrust minus the valve response time. Figure 12 shows the ignition delay plotted versus vacuum thrust level for a constant mixture ratio of 2.1±0.05. As the thrust level was decreased from approximately 10.6 N to 4.5 N, the ignition delay increased from 7.5 ms to 11.5 ms. Ignition delay versus mixture ratio, on the other hand, displayed no significant trend. Overall, ignition delay is very similar to that exhibited by the same thruster fired at normal operating temperatures (~22 °C) using MON-3 and MMH.

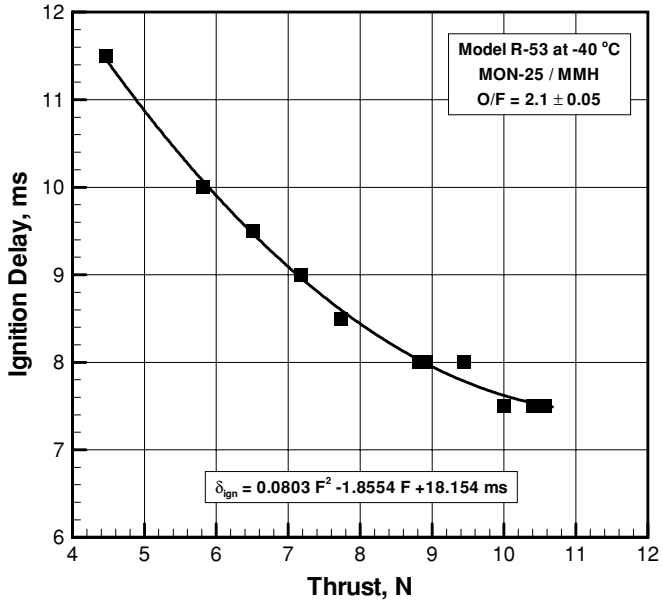

Figure 12 Ignition delay versus thrust.

At low thrust levels, roughly less than 6 N, the startup process exhibited a two-stage behavior. Immediately after ignition, the engine produced very little thrust, less than 1 N, for about 10 ms after which, the thrust abruptly reached its full steady state value. This delay in full combustion results in an accumulation of propellants followed by a detonation and a momentary spike in chamber pressure and thrust. The engine, however, was not damaged as a result of this phenomena.

3.2 Performance Mapping

Thirty-three 10-second hot firings were made at various thrust levels and mixture ratios to map the domain of performance for a range of inlet pressure with the engine and propellants conditioned to –40 °C. Initially, several trim runs were made to identify the nominal inlet pressures yielding an oxidizer-to-fuel mixture ratio, O/F, of 2.1 at a vacuum thrust level, F_{vac}, of 8.9 N. The nominal inlet pressures, p_{mo} and p_{mf}, were determined to be 1550 and 1830 kPa, respectively. Excursions from the nominal inlet pressures were such that, either the thrust was held constant at nominal while varying the mixture ratio or, *vice versa*. Performance data shown in the following plots and listed in Table 4 of the Appendix are averaged over the next-to-last second of each run.

Figure 13 shows a typical thrust trace for a 10-second hot firing. The thrust trace shown in Figure 13 was passed through a digital band-reject filter designed to eliminate both 60-Hz noise and thrust-stand ringing which would otherwise obfuscate the true engine thrust response. Figure 14 shows the power spectral density of the raw, unfiltered thrust signal, clearly identifying the 160-Hz natural frequency of the thrust-stand load cell and the 60-Hz line interference.

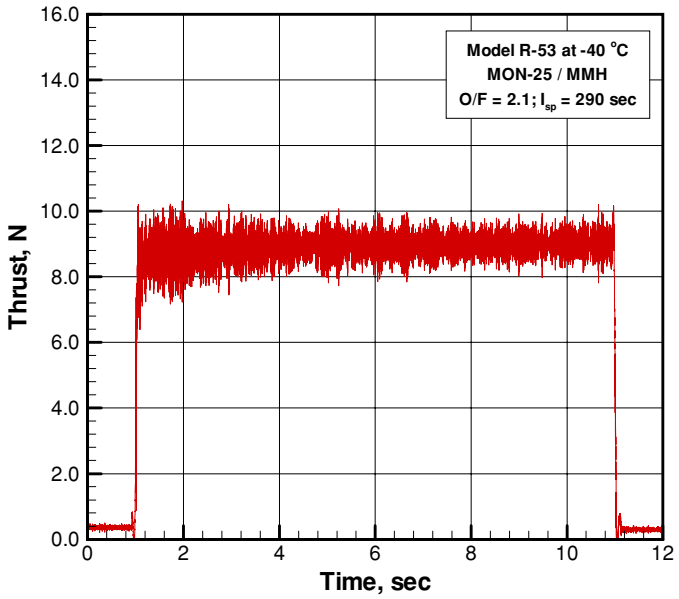

Figure 13 Typical filtered thrust trace for a 10-second run (Run #693).

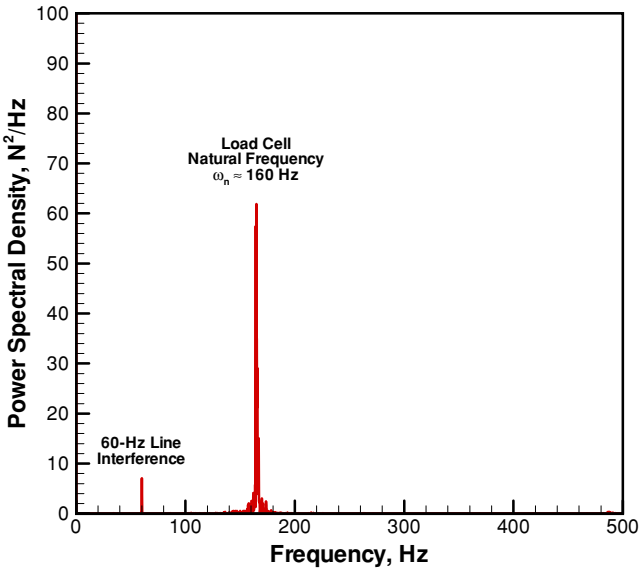

Figure 14 Typical power spectral density versus frequency of a raw thrust signal.

Figure 15 shows traces of the chamber and the injector-chamber interface temperatures, T_{ch}, and T_{c1} and T_{c2}, respectively. During hot fire, the chamber temperature increases monotonically and reaches a maximum of 1360 °C. Immediately after engine shutdown, T_{ch} decreases exponentially. Chamber temperatures below 900 °C could not be ascertained using the optical pyrometer and are, therefore, not plotted. Both injector-chamber interface temperatures increase very quickly over the first two seconds of hot firing then roll over and increase slowly throughout the entire run, reaching a maximum of 160 °C. After engine shutdown, both T_{c1} and T_{c2} increase and reach a maximum soak-back temperature of 290 °C after 7 seconds. Other engine temperature were not plotted because they showed no significant change over the 10-second firing duration.

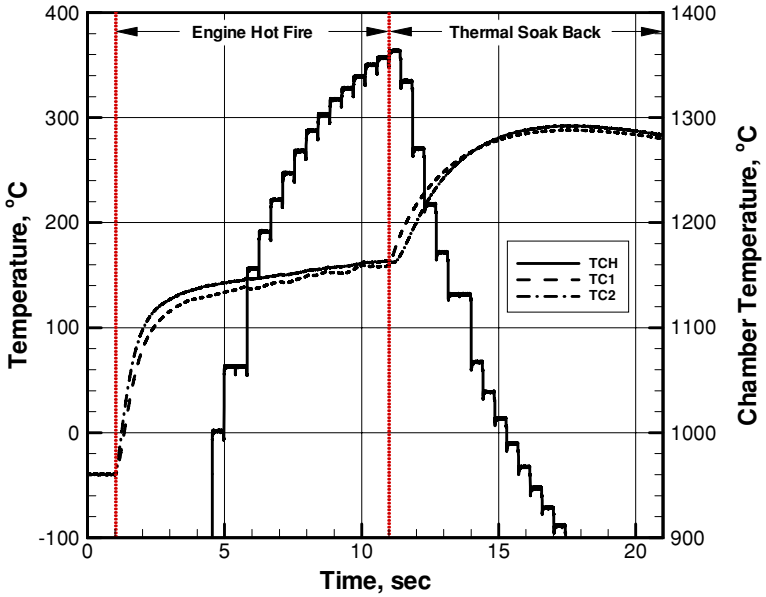

Figure 15 Typical thermal characteristics of a 10-sec hot fire; F = 8.9N, O/F = 2.2.

Figure 16 shows a plot of *C** efficiency versus vacuum thrust level for a constant mixture ratio of 2.1±0.05. The *C** efficiency is defined as the ratio of actual-to-theoretical characteristic velocities.

$$\eta_{C^*} = \frac{C^*_{actual}}{C^*_{theoretical}} \tag{1}$$

The *C** efficiency increased with thrust from 80.5% at 4.23 N to 93.0% at 10.2 N. For thrust levels above 8.5 N, the *C** efficiency appears to be relatively constant, however, it drops off sharply for thrust levels of less the 7 N. The empirical data was used to develop the following analytical curve fit for η_{C^*} as a function of thrust at an *O*/*F* of 2.1:

$$\eta_{C^*} = 0.0007630F^3 - 0.02205F^2 + 0.2150F + 0.2187; \quad 4.2\,\text{N} < F < 10.2\,\text{N}; \quad O/F = 2.1 \tag{2}$$

A chemical equilibrium computer code was used to determine the theoretical *C** values. The actual *C** values were calculated based on measured vacuum specific impulse, $I_{sp,vac}$, calculated thrust coefficient, and an assumed nozzle efficiency of 97%. The thrust coefficient along with the corresponding chamber pressure was determined iteratively using a chemical equilibrium and nozzle expansion code.

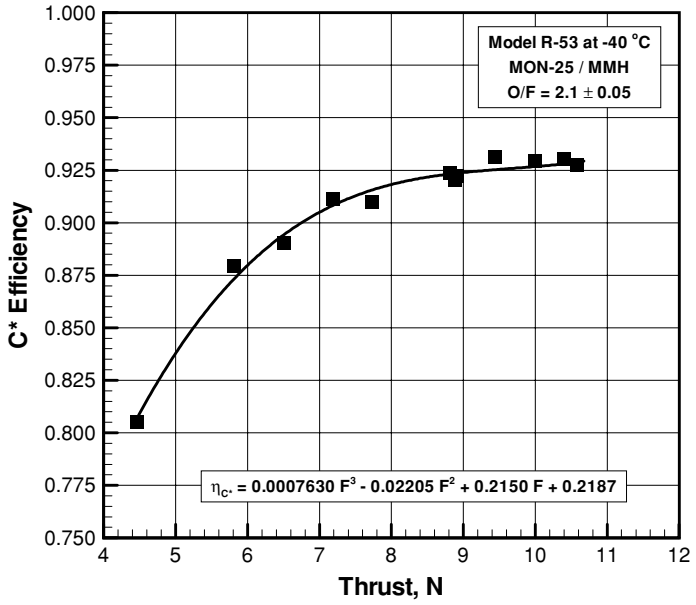

Figure 16 C* efficiency versus thrust.

Figure 17 shows C* efficiency as a function of the oxidizer-to-fuel mixture ratio, O/F, for a constant vacuum thrust level of 8.9±0.22 N. As the mixture ratio is increased, the C* efficiency initially increases from 92.6% at 1.61 to a maximum recorded value of 93.3% at 1.99 after which it decreases to 87.1% at 2.75. The experimental data was used to construct the following analytical curve fit for a thrust level of 8.9 N:

$$\eta_{C^*} = -0.0755(O/F)^2 + 0.2827(O/F) + 0.6629; \quad 1.61 < O/F < 2.75; \quad F = 8.9\text{N} \tag{3}$$

Using Eq. 3, the optimal mixture ratio is 1.87 producing an η_{C^*} of 92.8%, however, additional data is necessary to validate these values of regression analysis since the actual data show a maximum closer to 2.0.

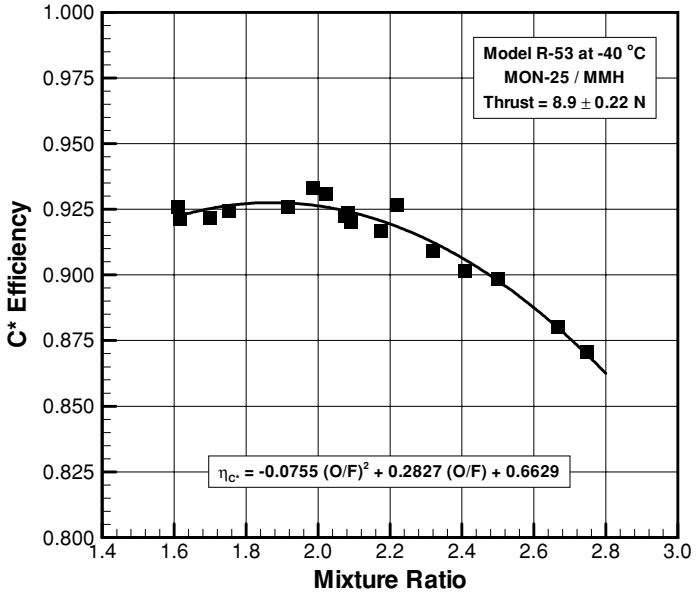

Figure 17 C* efficiency versus propellant mixture ratio.

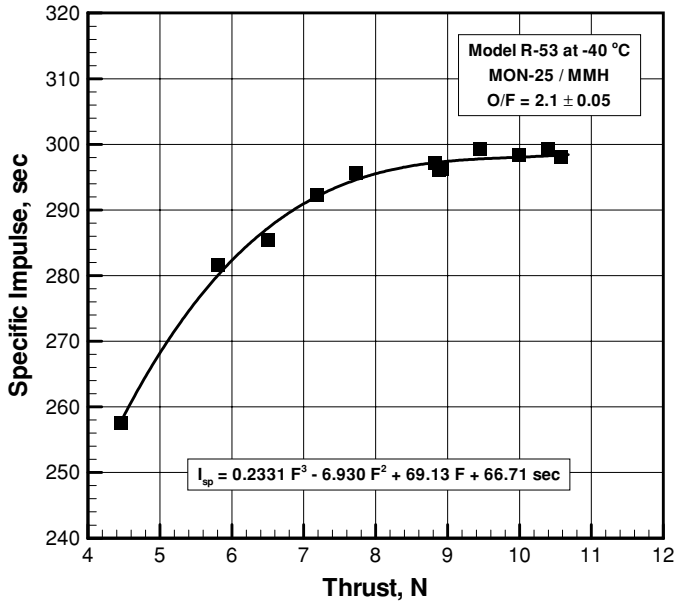

Figure 18 Specific impulse versus thrust.

Figure 18 shows a plot of vacuum specific impulse versus vacuum thrust for a constant mixture ratio of 2.1±0.05. Because the thrust coefficient is nearly constant at 1.84, the specific impulse is directly

proportional to the C^* efficiency and therefore shows the same trends. That is, as thrust increases, specific impulse also increases over the range tested. At 4.46 N of vacuum thrust, the measured I_{sp} was 257.6 sec, while at 10.58 N the I_{sp} was 298.1 sec. For thrust levels above 8.5 N, the specific impulse appears to be relatively constant, however, it drops off sharply for thrust levels of less the 7 N. The empirical data was used to construct the following analytical curve fit for an O/F of 2.1:

$$I_{sp} = 0.2331F^3 - 6.930F^2 + 69.13F + 66.71\,(\text{sec}); \quad 4.2\,\text{N} < F < 10.2\,\text{N}; \quad O/F = 2.1 \tag{4}$$

Figure 19 shows a plot of vacuum specific impulse as a function of the oxidizer-to-fuel mixture ratio, O/F, for a constant vacuum thrust level of 8.9±0.22 N. Again, because the thrust coefficient is nearly constant at 1.84, the specific impulse is directly proportional to the C^* efficiency and therefore shows the same trends. As the mixture ratio is increased, $I_{sp,vac}$ initially increases from 294.1 sec at 1.61 to a maximum recorded value of 300.7 sec at 1.99 after which it decreases to 271.1 sec at 2.75. The experimental data was used to construct the following analytical curve fit for a thrust level of 8.9 N:

$$I_{sp} = -41.559(O/F)^2 + 160.58(O/F) + 142.84\,(\text{sec}); \quad 1.61 < O/F < 2.75; \quad F = 8.9\text{N} \tag{5}$$

Using Eq. 3, the optimal mixture ratio is 1.93 producing an I_{sp} of 298.0, however, additional data is necessary to validate these values of regression analysis since the actual data show a maximum closer to 2.0.

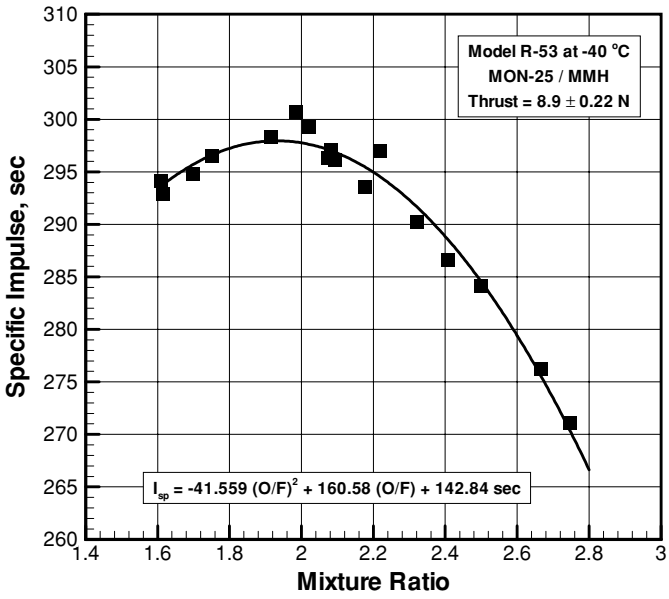

Figure 19 Specific impulse versus propellant mixture ratio.

Figure 20 shows as plot of chamber temperature averaged over the next-to-last second of each ten-second run versus vacuum thrust for a constant mixture ratio of 2.1±0.05. As thrust was increased from 4.46 N to 10.58 N, the chamber temperature increased from 993 °C to 1751 °C. This was to be expected as both the combustion efficiency and amount of total energy increase with thrust over the range of inlet pressures tested. The empirical data was used to construct the following analytical curve fit for an O/F of 2.1:

$$T_{ch} = -11.545F^2 + 297.7F - 105.7\ (\mathrm{K}); \quad 4.2\ \mathrm{N} < F < 10.2\ \mathrm{N};\ O/F = 2.1 \tag{4}$$

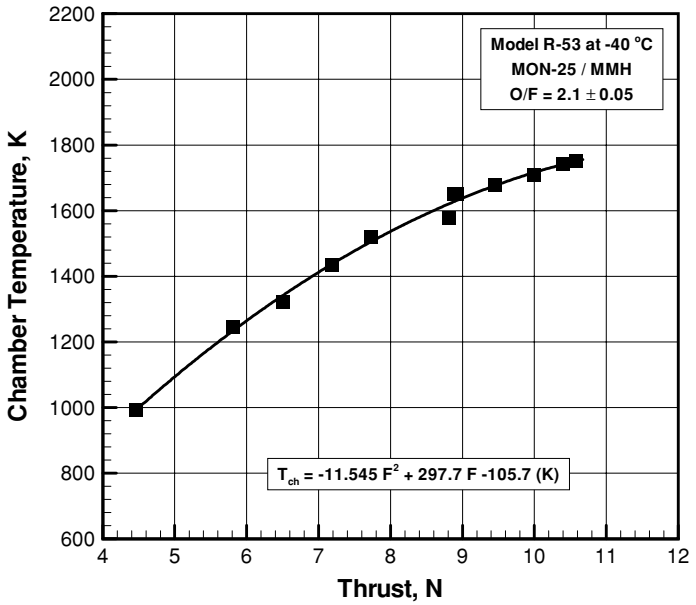

Figure 20 Chamber temperature versus thrust after 10 seconds of hot fire.

3.3 Steady-State Characteristics

The plot shown in Figure 21 displays the quasi-steady-state characteristics of the Model R-53. The term quasi-steady-state is used here, because, as indicated in the plot, the mixture ratio decreases with time and could not be held constant at its initial value of 2.1. The *O*/*F* does eventually, however, reach a steady value of approximately 1.82. For this mixture ratio, the injector-chamber interface temperatures, T_{c1} and T_{c2}, reach steady-state values of 145 and 180 °C, respectively. The chamber temperature reaches a steady-state value of 1420 °C.

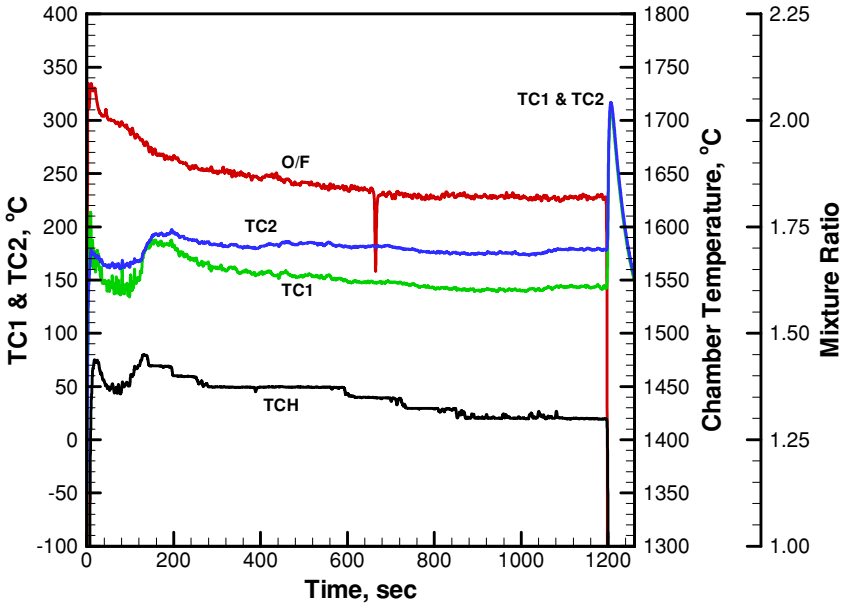

Figure 21 Quasi-steady-state thermal characteristics for a long-duration burn.

Figure 22 shows various temperature traces of the engine control valve and propellants for the same 1200-second burn shown in Figure 21. Note that the engine valve temperatures do not achieve steady state even after a 1200-sec burn. After 1200 seconds, the valve flange temperatures, T_{f1} and T_{f2}, are approximately 0 °C and the valve body temperatures, T_{vo} and T_{vf}, are approximately –12 °C. The propellant manifold temperatures, T_{mo} and T_{mf}, are shown for reference. It was not possible to maintain T_{mo} and T_{mf} at –40 °C for the entire duration of the run.

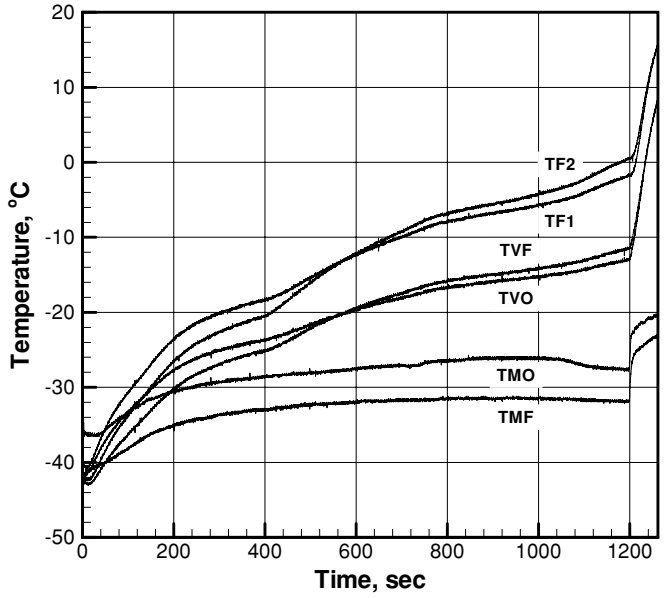

Figure 22 Engine control valve and manifold temperatures for a long-duration burn.

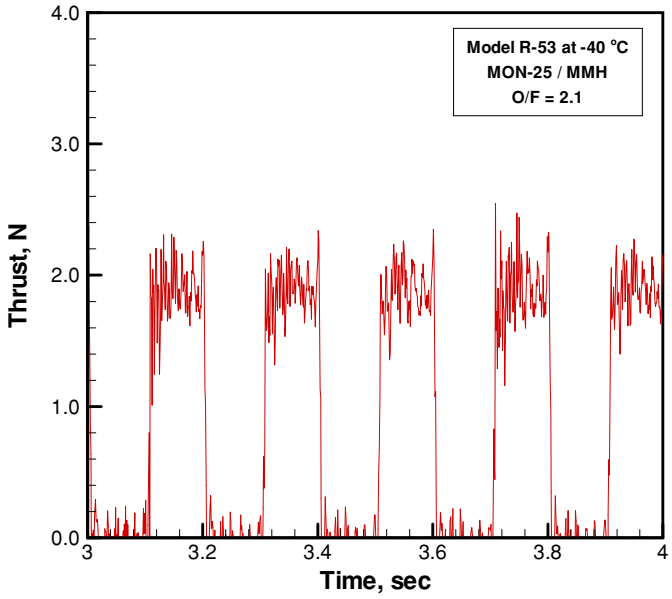

Figure 23 Several pulses from series of 20 with 50% duty cycle and a 0.2-sec period

3.4 Pulsing Performance

Figure 23 shows several typical pulses from a series of 20 with a 50% duty cycle and a 200-ms period (t_{on}/t_{off} = 0.1/0.1 seconds). After 20 pulses, the vacuum impulse bit reaches an average value of 0.22 N-s.

3.5 Performance at 1.4-kPa Cell Pressure

Although the engine was designed to operate in a vacuum environment, a single run was made to ascertain the performance of the engine at nominal inlet pressures with a cell pressure of 1.4 kPa. The idea was to simulate the average atmospheric pressure on the surface of Mars. It was expected that the flow inside the nozzle, designed for a much lower exhaust pressure, would separate and performance would drop off significantly. If the Model R-53 were to be flown within the atmosphere of Mars, the nozzle would have to be redesigned and optimized for the 1.5-kPa ambient pressure. In any event, a sixty-second run was made and results were obtained. Video recordings did indeed show nozzle flow separation well inside the nozzle. Table 3 shows a summary of the averages over the last second of the run.

Table 3 Summary of Performance at Elevated Cell Pressure

PARAMETER	VALUE	UNITS
Oxidizer inlet pressure	1547	kPa
Fuel inlet pressure	1826	kPa
Oxidizer inlet temperature	-31	°C
Fuel inlet temperature	-37	°C
Oxidizer flow rate	2.07	g/sec
Fuel flow rate	1.085	g/sec
Mixture ratio	1.9	
Thrust	7.7	N

Specific impulse	249.0	sec
Cell pressure	1.5	kPa
Chamber temperature	1443	°C

3.6 Vibration Characteristics

An accelerometer was attached to the back of the engine control valve to ascertain the system vibration characteristics. Figure 24 shows a typical accelerometer trace for the first 20.48 ms of a nominal 10-sec hot firing. The accelerometer had an accurate response range of up to 50,000 Hz with a resonant frequency of nearly 90,000 Hz. The data was sampled at 200,000 Hz using an IOTech high-speed data acquisition system. The highest-amplitude vibrations were experienced during the first 2 ms of startup after which the vibration was significantly reduced. There are momentary increases in the vibration amplitude, but they rarely exceed ±10 g.

Figure 25 shows the power spectral density versus frequency obtained from the accelerometer response trace shown in Figure 24.

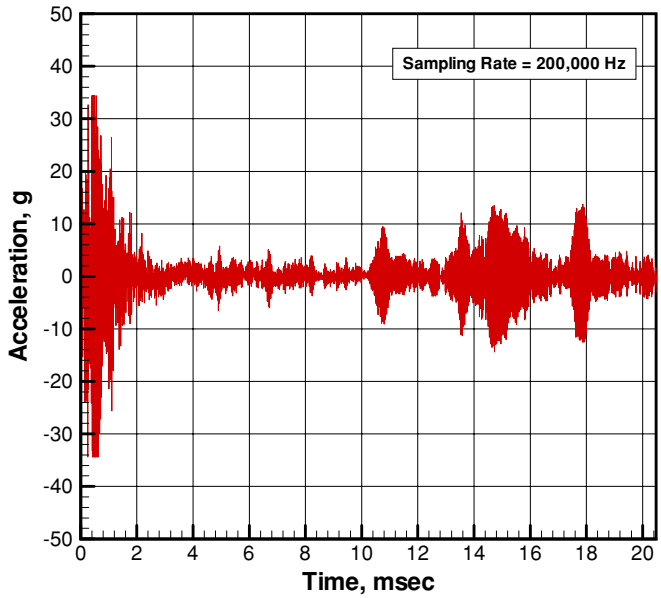

Figure 24 Accelerometer trace during first 20.48 ms of hot fire.

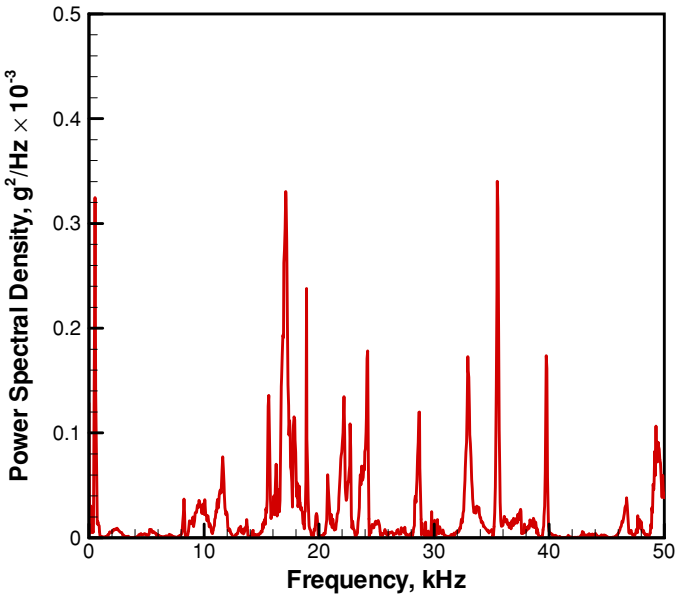

Figure 25 Power spectral density for the first 20.48 msec of hot fire.

4 NEW TECHNOLOGY

While no new technologies were developed within the scope of this effort, the technology demonstrated may be applied to other missions besides the Mars Flyer program. Test results show great promise for any power-limited space application where thermal management of the propulsion system may be restricted or even eliminated. Such missions include interplanetary travel, planetary descent and ascent, and intra-atmospheric planetary navigation.

5 SUMMARY AND CONCLUSIONS

An experimental investigation was conducted to assess the performance of an 8.9-N, bipropellant thruster operating at –40 °C with monomethylhydrazine (MMH) and mixed oxides of nitrogen (MON). To facilitate engine operation at low temperatures, dinitrogen tetroxide, N_2O_4, was saturated with nitric oxide, NO, to lower the freezing point. The freezing point of the industry-standard, 3% nitric oxide in dinitrogen tetroxide (MON-3) is -15 °C. By increasing the nitric oxide content to 25% (MON-25), the freezing point was lowered to –55 °C, thus enabling safe operation of the thruster at –40 °C with sufficient margin for error. The thruster was tested in a near-vacuum environment and conditioned, along with the propellants, to –40 °C prior to hot firing. Thruster operating parameters included oxidizer-to-fuel mixture ratios of 1.6 to 2.7 and inlet pressure ranging from 689 to 2070 kPa. The test matrix consisted of many 10-second firings and several 60, 300, 600, and 1200-second firings. Measurements included thrust, propellant flow rates, propellant inlet pressures and temperatures, engine temperatures, system vibrations, and valve control-signal characteristics. Data obtained from testing were analyzed to determine engine performance characteristics such as ignition delay, specific impulse, I_{sp}, versus oxidizer-to-mixture ratio, O/F, I_{sp} versus thrust, F, and the vibration frequency spectrum.

Although more data will be necessary to fully characterize the performance of the Model R-53 at –40 °C fired with MMH and MON-25, the following general statements can be made.

- The engine was successfully operated at a thrust level of 8.9-N and –40 °C when fired with MMH and MON-25.
- Performance is comparable to operation at normal temperatures (22 °C) with MMH and MON-3.
- At nominal inlet pressures, the ignition delay is approximately 8 ms, which is comparable to operation at normal temperatures with MMH and MON-3.
- Based on regression analyses, optimal performance for the 8.9-N thruster will be obtained at an O/F of 1.93 with an anticipated average specific impulse of 298 sec.
- The thruster accumulated nearly 10,000 seconds of operation without failure.
- For a duty cycle of 50% with a 200-ms period, the average vacuum impulse bit was 0.22 N-sec
- The thruster was successfully operated in an atmosphere of 1.5 kPa.
- The thruster exhibits no detrimental vibrations during hot firing.

APPENDIX

Summary Data Listings

Table 4 Performance Summary Data for 10-second Hot Firings.

RUN	P_{mo}	P_{mf}	T_{mo}	T_{mf}	w_o	w_f	O/F	F	P_{cell}	F_{vac}	$I_{sp,vac}$	T_{ch}	C*	C_f	P_c	δ
	kPa	kPa	°C	°C	g/sec	g/sec		N	Pa	N	sec	°C	m/sec		kPa	ms
688	1571	1565	-35.7	-41.3	2.196	0.855	2.57	8.36	73.1	8.50	284.0	1377	1500	1.857	595.9	8.0
689	1570	1555	-36.1	-41.3	2.223	0.840	2.65	8.14	88.0	8.30	276.4	1279	1459	1.858	581.9	8.0
690	1567	1586	-37.9	-44.2	2.218	0.856	2.59	8.12	104.7	8.32	276.0	1308	1458	1.857	583.7	8.0
691	1566	1658	-37.9	-46.7	2.163	0.878	2.46	8.27	111.7	8.48	284.5	1324	1505	1.854	596.0	8.0
692	1564	1795	-38.0	-37.2	2.125	0.977	2.18	8.79	76.5	8.93	293.6	1385	1558	1.847	629.6	8.0
693	1543	1836	-38.6	-39.3	2.071	0.998	2.07	8.73	100.9	8.92	296.3	1379	1576	1.844	630.0	8.0
694	1549	1828	-37.8	-39.3	2.070	0.989	2.09	8.74	77.6	8.88	296.1	1377	1575	1.844	627.4	8.0
695	1550	1904	-38.4	-39.9	2.035	1.025	1.99	8.82	109.8	9.02	300.7	1375	1603	1.839	639.1	8.0
696	1576	2022	-39.0	-39.9	2.048	1.070	1.92	8.99	69.6	9.12	298.3	1379	1594	1.835	647.3	8.0
697	1522	2076	-37.0	-38.9	1.977	1.129	1.75	8.79	125.1	9.03	296.5	1343	1595	1.823	645.2	8.0
698	1479	2108	-38.7	-39.6	1.928	1.134	1.70	8.69	85.8	8.85	294.8	1313	1590	1.818	634.2	8.0
699	1447	2134	-37.8	-38.6	1.868	1.160	1.61	8.51	116.9	8.73	294.1	1279	1594	1.809	629.0	8.0
700	1449	2177	-38.1	-39.5	1.889	1.169	1.62	8.51	145.8	8.78	292.9	1273	1587	1.810	632.3	8.0
701	1621	1766	-38.2	-40.1	2.125	0.957	2.22	8.79	97.1	8.98	297.0	1352	1576	1.849	632.5	8.0
702	1657	1729	-37.3	-39.6	2.202	0.949	2.32	8.74	121.5	8.97	290.2	1341	1538	1.851	631.0	8.0
703	1657	1693	-37.3	-39.7	2.226	0.924	2.41	8.69	87.5	8.85	286.6	1332	1517	1.853	622.3	8.0
704	1657	1622	-37.3	-39.7	2.232	0.893	2.50	8.46	129.6	8.71	284.1	1306	1502	1.855	611.3	8.0
705	1695	1559	-38.2	-40.5	2.301	0.863	2.67	8.31	107.5	8.51	274.4	1311	1447	1.859	596.4	8.0
706	1727	1591	-38.6	-41.2	2.325	0.872	2.67	8.40	138.9	8.66	276.2	1318	1457	1.859	606.7	8.0
707	1824	1629	-39.1	-40.7	2.425	0.883	2.75	8.57	116.9	8.79	271.1	1320	1434	1.854	617.7	8.0
708	1553	1835	-39.1	-40.2	2.028	1.003	2.02	8.71	99.1	8.90	299.3	1360	1596	1.840	629.9	8.0
709	1696	1971	-39.3	-39.8	2.171	1.046	2.07	9.17	147.1	9.45	299.3	1403	1593	1.842	667.9	8.0
710	1861	2108	-39.8	-40.5	2.331	1.086	2.15	9.73	140.7	10.00	298.4	1436	1585	1.846	705.3	7.5
711	1967	2248	-40.2	-40.6	2.411	1.134	2.13	10.20	108.9	10.40	299.2	1471	1590	1.846	734.0	7.5
713	2028	2315	-40.4	-40.8	2.468	1.150	2.15	10.41	88.4	10.58	298.1	1478	1584	1.846	746.3	7.5
714	1407	1697	-40.4	-41.1	1.868	0.920	2.03	8.03	84.0	8.19	299.4	1299	1594	1.842	579.1	8.5
715	1306	1555	-40.2	-41.7	1.803	0.863	2.09	7.52	111.1	7.73	295.6	1246	1572	1.844	545.8	8.5
716	1202	1416	-41.3	-42.2	1.705	0.801	2.13	6.92	138.0	7.18	292.3	1162	1553	1.846	506.8	9.0
717	1072	1278	-41.1	-42.3	1.580	0.744	2.12	6.28	121.6	6.51	285.5	1050	1517	1.846	459.2	9.5
718	929	1105	-39.8	-40.7	1.427	0.677	2.11	5.64	87.3	5.81	281.5	971	1496	1.845	410.1	10.0
719	792	963	-38.8	-40.2	1.270	0.632	2.01	4.87	122.4	5.10	273.4	727	1457	1.841	360.7	11.0
720	723	848	-38.8	-40.2	1.191	0.575	2.07	4.23	125.2	4.46	257.6	721	1370	1.844	315.3	11.5
721	1551	1831	-39.8	-39.6	2.044	0.982	2.08	8.64	92.7	8.82	297.1	1304	1580	1.844	622.9	8.0

REPORT DOCUMENTATION PAGE

Form Approved
OMB No. 0704-0188

1. AGENCY USE ONLY (*Leave blank*)	2. REPORT DATE	3. REPORT TYPE AND DATES COVERED
	April 2001	Final Contractor Report

4. TITLE AND SUBTITLE

Mars Flyer Rocket Propulsion Risk Assessment
Kaiser Marquardt Testing

5. FUNDING NUMBERS

WU–755–B4–01–00
NAS3–99198

6. AUTHOR(S)

Kaiser Marquardt

7. PERFORMING ORGANIZATION NAME(S) AND ADDRESS(ES)

Kaiser Marquardt
Rocket Propulsion Systems
16555 Saticoy Street
Van Nuys, California 91406–1739

8. PERFORMING ORGANIZATION REPORT NUMBER

E–12643

9. SPONSORING/MONITORING AGENCY NAME(S) AND ADDRESS(ES)

National Aeronautics and Space Administration
Washington, DC 20546–0001

10. SPONSORING/MONITORING AGENCY REPORT NUMBER

NASA CR—2001-210710

11. SUPPLEMENTARY NOTES

Kaiser Marquardt has been acquired by General Dynamics, Ordinance and Tactical Systems, Aerospace Operations, 11441 Willows Road N.E., P.O. Box 97009, Redmond, WA 98073-9709. Project Managers, Brian Reed, 216–977–7489, and James Biaglow, 216–977–7480, Power and On-Board Propulsion Technology Division, NASA Glenn Research Center, organization code 5430.

12a. DISTRIBUTION/AVAILABILITY STATEMENT

Unclassified - Unlimited
Subject Category: 20 Distribution: Nonstandard

Available electronically at http://gltrs.grc.nasa.gov/GLTRS

This publication is available from the NASA Center for AeroSpace Information, 301–621–0390.

12b. DISTRIBUTION CODE

13. ABSTRACT ***(Maximum 200 words)***

This report describes the investigation of a 10-N, bipropellant thruster, operating at –40 ˚C, with monomethylhydrazine (MMH) and 25% nitric oxide in nitrogen tetroxide (MON-25). The thruster testing was conducted as part of a risk reduction activity for the Mars Flyer, a proposed mission to fly a miniature airplane in the Martian atmosphere. Testing was conducted using an existing thruster, designed for MMH and MON-3 propellants. The nitric oxide content of MON-3 was increased to 25%, to lower its freezing point to –55 ˚C. The thruster was conditioned, along with the propellants, to temperature prior to hot firing. Thruster operating parameters included oxidizer-to-fuel mixture ratios of 1.6 to 2.7 and inlet pressure ranging from 689 to 2070 kPa. The test matrix consisted of many 10-second firings and several 60-, 300-, 600-, and 1200-second firings, as well as pulse testing. The thruster successfully accumulated nearly 10,000 seconds of operation without failure, at temperatures ranging from –40 ˚C to 22 ˚C. At nominal inlet pressures, the ignition delay was comparable to MMH/MON-3 operation. The optimal performance for the 8.9-N thruster was determined to be at a mixture ratio of 1.93 with an average specific impulse of 298 sec.

14. SUBJECT TERMS

Liquid rocket propellants; Rocket testing; Mixed oxides of nitrogen; Mars flyer

15. NUMBER OF PAGES
35

16. PRICE CODE
A03

17. SECURITY CLASSIFICATION OF REPORT	18. SECURITY CLASSIFICATION OF THIS PAGE	19. SECURITY CLASSIFICATION OF ABSTRACT	20. LIMITATION OF ABSTRACT
Unclassified	Unclassified	Unclassified	